

Expert Router: Orchestrating Efficient Language Model Inference through Prompt Classification

Josef Pichlmeier *
BMW Group
Ludwig Maximilians Universität

Philipp Ross
BMW Group

Andre Luckow
BMW Group
Ludwig Maximilians Universität

Abstract—Large Language Models (LLMs) have experienced widespread adoption across scientific and industrial domains due to their versatility and utility for diverse tasks. Nevertheless, deploying and serving these models at scale with optimal throughput and latency remains a significant challenge, primarily because of the high computational and memory demands associated with LLMs. To tackle this limitation, we introduce Expert Router, a system designed to orchestrate multiple expert models efficiently, thereby enhancing scalability. Expert Router is a parallel inference system with a central routing gateway that distributes incoming requests using a clustering method. This approach effectively partitions incoming requests among available LLMs, maximizing overall throughput. Our extensive evaluations encompassed up to 1,000 concurrent users, providing comprehensive insights into the system’s behavior from user and infrastructure perspectives. The results demonstrate Expert Router’s effectiveness in handling high-load scenarios and achieving higher throughput rates, particularly under many concurrent users.

Index Terms—Large Language Models, Performance, Throughput

I. INTRODUCTION

Foundation models, particularly large language models (LLMs) like GPT-4 [1], Claude 3 [2], and Llama 2 [3] offer versatile applications across diverse industrial and scientific domains [4], such as the automotive domain [5], software development [6], physics [7], and medicine [8]. LLMs and their underlying transformer architecture [9] have been used in solving many natural language processing problems including sentiment analysis [10] and classification. More recently generative tasks such as summarization, text generation, and conversational systems are a dominant field of application. Many of these tasks demand multiple LLM inferences, e. g., to execute complex prompt sequences derived from different prompt engineering approaches [11], to utilize data integrations via retrieval augmentation generation, or to orchestrate agent-based workflows for optimal results [12].

The need to efficiently conduct inference and serve these models is critical to enable these applications. However, the deployment of LLMs presents significant challenges. This includes the complex model architecture and addressing their high computational and memory demands, which often necessitates specialized hardware like GPUs. For larger models, e. g., models beyond 70 billion parameters, it is required to

partition the model across multiple GPUs utilizing model parallelism (e. g, tensor, and pipeline parallelism) or other optimization methods (e. g., pruning and quantization).

Smaller models can easily fit into the memory of a single GPU and do not require expensive multi-node tensor parallelism. Thus, such small models have recently received increased attention from industry and research. For example, Chinchilla models [13] prioritize training on more tokens rather than increasing the number of parameters, thus optimizing compute to achieve smaller yet higher-performing models. Other small language models, e. g., Phi-2, utilize high-quality training data [14]. Furthermore, using a Mixture of Experts (MoE), i. e. models that partition parameters into experts, each with unique weights, avoid the need to utilize all weights during training and inference [15] (e. g., Mixtral [16]). Other approaches utilize multiple independent smaller expert models and couple them hierarchically (e. g., Tabi [17]) or using other routing and coordination approaches.

Gururangan et al. [18] introduced the Cluster-Branch-Train-Merge (c-BTM) technique, which employs unsupervised clustering using k-means to partition a given dataset into distinct domains as the basis for multiple expert models that are trained in parallel. During inference, only experts relevant to the topic of the incoming prompt are utilized. We extend Gururangan’s work to new modern LLM models, such as Llama 2, and focus on characterizing the inference performance. For this purpose, we investigate C-BTM’s ensemble of expert approaches and compare them to the inference of larger parameter models using throughput and latency.

In this work, we introduce *Expert Router*, an inference system for expert model ensembles. Expert Router is designed for an ensemble of expert systems. It integrates with state-of-the-art inference systems, particularly TensorRT-LLM and Triton. Our modular system design is capable of integrating various models and inference systems. We evaluate Expert Router using extensive experimentation involving up to 1000 concurrent users and assess the system performance from user and system perspectives.

We summarize our contributions in this work as follows:

- We introduce a highly modular architecture called Expert Router that allows us to orchestrate multiple expert models efficiently.
- We investigate several configurations of Expert Router, including quantized and non-quantized state-of-the-art

*Josef.Pichlmeier@bmw.de

LLMs. These configurations are benchmarked against a baseline model on a diverse set of metrics grouped into user and system perspectives.

- We conduct an extensive evaluation of all architectures with up to 1,000 concurrent users, in total producing over one billion response tokens to prove Expert Routers’ effectiveness in handling high-load scenarios.

II. RELATED WORK

Efforts to improve LLM serving can be grouped into two main categories: algorithmic innovations and system optimization [19]. In this section, we survey the techniques developed within these categories as well as for benchmarking these systems.

A. LLM Algorithmic Innovations

Recently, MoE models have gained much attention due to their high performance in various benchmarks [16], [20]–[23]. MoE models can be classified into two categories: integrated experts and ensembles of experts. An integrated MoE model uses a router network in specific layers to incorporate the output of distinct parameter groups, the experts. Ensembles of experts rely on separate models that are independently trained. All or a subset of these models are activated during inference, and the outcome—either the final output or the output activity of specific layers—is averaged.

An example of an integrated MoE model is Mixtral, which consists of eight seven-billion-parameter models [21]. It outperforms state-of-the-art classical LLM architecture in several benchmarks, such as LLama2, GPT-3.5, or Gemini Pro [21].

Gurungan et al. [18] propose an ensemble of expert approach called c-BTM. This technique involves training sparse language models on text corpora with minimal inter-node communication. It achieves this by clustering text corpora into related topics and training a dedicated expert language model for each cluster. Once trained, these models are collectively utilized for prediction tasks. We adopt the k-means clustering algorithm used and refined by Gururangan et al. to schedule incoming prompts in our architecture, leveraging their results for our model orchestration framework.

Another example of an ensemble of experts is OrchestraLLM [24]. This approach uses small and large language models for dialogue state tracking. OrchestraLLM’s dynamic routing mechanism for dialogue state tracking involves evaluating each input instance to decide the best-fit language model for processing. This process starts by calculating the semantic embedding of the input. Then, it compares this embedding with semantic representations from various expert pools using a cosine distance measure. The system then routes the input to the appropriate expert model based on a majority vote from these comparisons.

B. LLM System Optimization

In addition to optimizing the core architecture of LLMs, improving the efficiency of inference calculations by optimizing the model deployment is possible. A key strategy in

this domain involves modifying the memory storage format of model weights, activation, and user context, which is known as quantization [19]. Thereby, the general architecture is left unchanged, and only the data format is altered [25]. Various methods exist that allow transforming parameters that have been initially stored in FP32 or FP16 format to lower resolution storage formats such as FP8, INT8, INT4 or even INT2 [26]–[30]. For many of these Post Training Quantization (PTQ) techniques, it is possible to develop efficient GPU kernels [27]. This translates into reduced memory requirements and can lead to measurable latency reductions in certain settings [31].

Besides quantization techniques, the parallelization of models significantly influences the inference efficiency [32], [33]. A common approach called tensor parallelization distributes one LLM across multiple GPUs on the same node. Weight matrices are sliced and distributed across different GPUs depending on the implementation. Each GPU evaluates the corresponding matrix multiplication independently, and the final result can be derived with only little communication overhead. Another degree of parallelization is called pipeline parallelization, where different layers of the network are evaluated on different GPUs [34].

Wang et al. [17] proposed the “Tabi” multi-level inference system for coordinating multiple small models and more complex LLMs using dynamic routing techniques. The core idea is to use less resource-intensive models for more straightforward queries instead of employing an LLM for every task.

The last layer in the system stack is formed by the software framework used to deploy the models. These programs often come with pre-set batching and scheduling techniques and optimized kernels for transformer architectures [19]. Examples are vLLM, ONNX Runtime, NVIDIA Triton, TorchServe, DeepSpeed Inference and HuggingFace text generation [35]–[40].

One approach to optimize LLM serving specifically targeting the batching mechanism has been introduced by Agrawal et al. [41]. Their work segments the inference process into two distinct phases: prefill and decode. The prefill phase is optimized for parallel processing, fully engaging GPU computational power, but at the expense of higher latency. Conversely, the decode phase processes output tokens sequentially, not fully utilizing the available GPU compute. This creates the challenge of balancing high throughput and low latency in LLM serving systems. Agrawal et al. have developed Sarathi-Serve, an inference scheduler that employs chunked-prefills and stall-free scheduling to address this issue.

C. Benchmarking of Inference Architectures

Performance characteristics can be assessed from two perspectives: system and user. On the system side, an important metric is throughput, defined as the number of tokens generated by the LLM per second [19]. From the user’s viewpoint, several metrics beyond throughput are relevant, including first-token response time, inter-token latency, and total processing time [42].

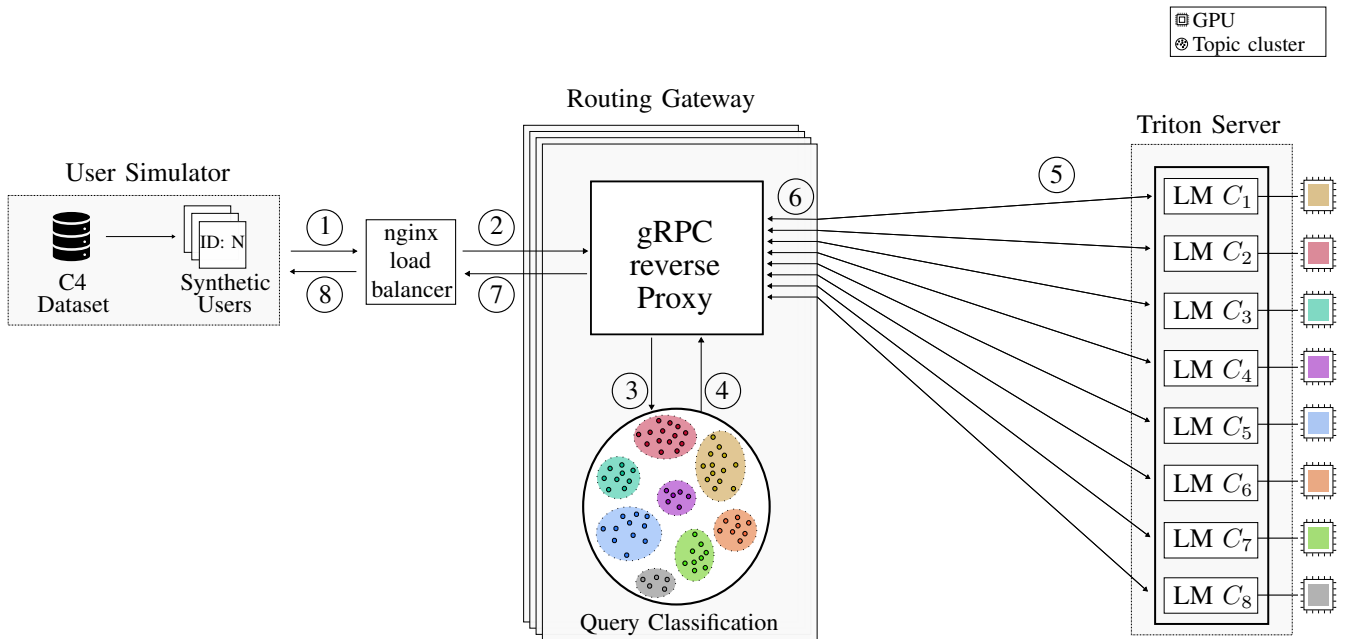


Fig. 1. **Expert router architecture and experimental setup:** The architecture comprises three main components: the routing gateway, the Triton inference server, and the user simulator. Incoming prompts (1) are classified by the routing gateway using a k-means algorithm (2 + 3) and forwarded to the corresponding language model (4). All models run on different GPUs independently and can process queries concurrently. The inference responses are returned to the respective users (5 + 6). The clustering algorithm has been trained on a set of samples indicated by the dots, and new prompts are classified according to the respective topics indicated by the colors.

As stated by Miao et al., creating a holistic evaluation framework that measures the performance of LLM inference systems is complicated due to the large configuration space of the underlying architectures [19]. Recently, MLPerf has added a GPT-J test scenario to their benchmarking suite where it is possible to evaluate the number of samples and queries per second [43], [44]. Another benchmarking framework that has lately received significant attention from the community is LLMPerf, which Anyscale developed. Their platform allows measuring key characteristics such as first token response time, throughput, inter-token latency etc. [42], [45].

Our work builds upon these approaches for model optimization and deployment, directly addressing the challenge of coordinating multiple expert models efficiently. For this, we are employing the k-means cluster algorithm developed by Gurungan et al. for routing user prompts to the matching expert model [18]. Therefore, our approach differs from the traditional MoE methodology by not averaging any activation outputs but rather activating models individually. Each model in our approach is fully autonomous, generating its own distinct output. This architectural choice is motivated by the flexibility it introduces, allowing for the extension to appropriate domains. Another key strength is its ability to incorporate many optimization techniques, such as system optimizations and algorithmic innovations. Its modular design ensures that components can be seamlessly integrated or updated. Our work differentiates itself from a classical data parallel architecture, as we do not statically but dynamically route incoming prompts based on their topic. To thoroughly evaluate our

architecture, we employ many of the aforementioned metrics.

III. SYSTEM ARCHITECTURE

This section presents Expert Router’s architecture, which enables efficient and scalable LLM inference. The architecture is highly modular, i.e., individual components can be replaced or upgraded, allowing for continuous and systematic improvements. For example, the architecture enables LLMs to be individually updated without necessitating a complete system update. Expert Router can be deployed in a heterogeneous computing environment irrespective of the hardware components’ manufacturing era.

Figure 1 illustrates the system architecture. The routing gateway is the central component of the system. It manages request distribution to the inference servers. Specifically, we utilize NVIDIA Triton [37] and TensorRT-LLM [46] to execute the inference tasks. The system can easily be scaled on every layer, e.g., utilizing a load balancer like NGINX before the routing gateway or adding new Triton server instances. It utilizes the gRPC protocol [47] for communication between these components. Expert Router can achieve high throughputs through this design while providing a flexible solution for LLM inference.

A. Routing Gateway

The routing gateway acts as an intermediary; it receives and distributes requests across inference servers. This functionality is also referred to as reverse proxy. After receiving a new inference request, the routing gateway extracts the user prompt.

It sends it to the query classification (Step 3/4 in Figure 1), where a k-means clustering algorithm is used to determine the target cluster of the prompt. This mechanism is directly adopted from the system developed by Gururangan et al. [18].

We follow the original paper’s preprocessing steps: excluding stop-words and substituting numerical tokens. The clustering process transforms the prompt text data using a TF-IDF vectorizer from the scikit-learn library [48]. The TF-IDF vectors are then condensed to 100 dimensions via a singular value decomposition. This dimensionality reduction is followed by a normalization step by subtracting the mean and scaling the vectors to unit variance [18]. We employ the same custom PyTorch implementation, including the weights of the k-means model published by [18], which has been trained on a selected portion of the C4 dataset [49].

Expert Router uses the pre-trained k-means model to classify the prompt into an appropriate cluster when receiving a new prompt. The routing gateway then directs the prompt to the designated language model hosted on a Triton server instance. To increase prompt classification throughput, we are deploying 16 routing gateway instances in combination with an NGINX load balancer that distributes the incoming requests in a round robin mechanism [50] (Step 1/2 and 7/8 in Figure 1).

B. Inference Backend and Triton Server

Following an overview of large language model (LLM) inference techniques, we discuss the particular inference backend employed by Expert Router: the GPU-accelerated NVIDIA Triton server.

LLM Inference: We rely on advanced inference techniques, particularly optimization for the self-attention mechanisms and batching. Self-attention enables every token of the input sequence to be evaluated against all preceding tokens, thereby creating a contextual representation. This process starts by converting input tokens into Query (Q), Key (K), and Value (V) vectors through trained weights. Next, it calculates the dot products between all Q and K vectors and applies a softmax function. The outcome of this calculation is combined with the V vectors through another dot product to produce a weighted sum. This weighted sum models the context between tokens.

Multi-head attention enables transformers to leverage multiple attention mechanisms simultaneously, with each “head” focusing on distinct representation subspaces. These heads independently compute attention weights for the Q, K, and V vectors. By aggregating the outputs of these heads, multi-head attention allows the capture of a broader range of relationships within the data. Further, this allows for parallelized examination of input sequences [9].

A critical optimization within this process is the use of a KV-cache. This cache stores the K and V vectors from previous computations, eliminating the need for redundant recalculation [41].

In inference scenarios of LLMs, there are two main processing stages. The first stage is known as the prefill phase. During this phase, the system processes the entire input sequence to

produce the first output token, simultaneously populating the KV-cache with K and V vectors derived from the input. This stage primarily relies on matrix-matrix parallelization, which can be efficiently parallelized [41].

Following the prefill phase, new tokens are generated autoregressively, leveraging the precomputed activations stored in the KV-cache. This is called the decode phase. The decoding phase is computationally less demanding, often underutilizing the GPU [41]. To address this inefficiency, employing batching techniques becomes essential for optimizing LLM service, especially in high-load scenarios.

There are two primary batching techniques: static and continuous batching, also called in-flight batching. Static batching aggregates all requests and processes them together until each has received a complete response. In contrast, continuous batching allows requests to dynamically join or leave the processing queue at each model iteration [51]. One iteration is the generation of a response token for all requests in the batch. We use in-flight batching for all models deployed on the Triton server to maximize throughput.

Triton Server: We use NVIDIA’s Triton server as an inference backend. The Triton server starts with the inference process after receiving the prompt from the routing gateway (Step 5 in Figure 1). Each model is hosted on a dedicated Triton server, with each server assigned to its own GPU. This configuration allows the system to individually address models via distinct ports, each linked to a specific cluster identified by the k-means clustering algorithm. This architectural choice eliminates the need for communication between different models or GPUs, as each Triton server is equipped with its scheduling and in-flight batching mechanisms. We use each Triton server in streaming mode, i. e., tokens generated by the model are instantly transmitted back to the routing gateway, avoiding any buffering of tokens on the system side (Step 6 in Figure 1). The routing gateway then forwards these tokens to the end-users through the NGINX load balancer (Steps 7/8 in Figure 1).

To enhance inference performance, we utilize TensorRT-LLM, a specialized framework designed to build and deploy LLM engines. TensorRT-LLM is optimized for NVIDIA hardware, ensuring that state-of-the-art models such as LLama2, Mixtral, and Gemini can operate efficiently.

IV. EXPERIMENTAL SETUP

This section introduces the experimental setup for inference testing, including a description of the models employed within the Expert Router and the chosen baseline model. It also describes the approach for simulating high-load scenarios by increasing the number of concurrent users, realized through the User Simulator in Figure 1. These experiments aim to assess the Expert Router’s performance and benchmark it against a high-throughput baseline model.

A. Model deployment

This study utilizes LLama 2 models [3] across all experiments. All experiments are conducted on a DGX H100 system

with eight H100 GPUs. Each of them features 80 GB of GPU memory. The experimental framework is given by two primary scenarios: one involving runs utilizing a baseline model and the other our Expert Router architecture.

The aim is to evaluate the Expert Router’s performance by benchmarking it against a baseline model optimized for high throughput. This baseline model is a Llama 2 configuration with 70 billion parameters (70B), tensor parallelized over eight GPUs, and FP16 weights.

A) *70B FP16 TP8*: As outlined in Table I, the baseline model operates with a large batch size of 600, optimized to maximize throughput. For the baseline results, the user requests are directly sent to the Triton inference server hosting the tensor-parallel 70B model without the routing gateway and load balancer as intermediate layers.

TABLE I
KEY SPECIFICATIONS OF THE MODELS FOR ALL EXPERIMENTS CONDUCTED WITHIN THIS STUDY, LLAMA 2 MODELS ARE USED. BESIDES THE BATCH SIZE, THE TABLE LISTS MEMORY-RELATED SPECIFICATIONS FOR EACH OF THE MODELS, SUCH AS THE WEIGHT AND THE KV-CACHE SIZE IN GB.

Model \ Specs	Weights	KV-cache	Batch size
Baseline Model			
A) 70B FP16 TP8	141 GB	366 GB	600
Orchestrated Models			
B) 70B INT8 (Exp. Router)	69 GB	12 GB	60
C) 13B FP16 (Exp. Router)	26 GB	54 GB	40
D) 13B FP8 (Exp. Router)	13 GB	65 GB	150

Our research examines the impact of varying model specifications and configurations on system performance for the models integrated within the Expert Router. Specifically, we investigate three configurations: the first (B) uses eight quantized 70B models to explore high-parameter scenarios; the second (C) involves eight 13 billion parameters (13B) models, allowing for a larger KV-cache and FP16 weights; and the third (D) employs eight 13B models optimized for the H100 hardware using FP8 format. With every specification, our objective is to optimize the batch size within the constraints of available GPU memory, ensuring maximal utilization.

B) *70B INT8 (Exp. Router)*: The first configuration uses a Llama 2 70B model with INT8 quantized weights and KV-cache. We employ weight-only quantization provided within the TensorRT-LLM library [46] to build the model. Table I shows that the resulting model uses 69 GB of GPU memory for its weights and 72×10^3 tokens in the KV-cache, allocating 12 GB of GPU memory. The batch size is set to 60. Each GPU hosts a single INT8 70B model in this experiment, leading to 560 billion INT8 quantized weights across the system. In our tests, we included this particular model setup to explore how

the Expert Router performs when handling models with many parameters.

C) *13B FP16 (Exp. Router)*: The second configuration uses a Llama 2 13B model, requiring 26 GB for weight storage. This reduction in memory requirement for weights allows allocating a greater portion of available GPU memory to the KV-cache. In this instance, the KV-cache accommodates 160×10^3 tokens. This allows for the evaluation of the Expert Router’s performance with non-quantized models that leverage a larger KV cache.

D) *13B FP8 (Exp. Router)*: Lastly, we deploy a quantized version of the 13B model, with both weights and the KV-cache formatted in FP8. We utilized the NVIDIA Algorithmic Model Optimization (AMMO) toolkit for weight quantization, part of TensorRT-LLM [46]. This approach allows us to explore the impact of an expanded KV-cache on system performance and leverage the computational efficiency offered by the NVIDIA H100’s enhanced support for FP8 matrix multiplications [52]. In this setup, each model accommodates approximately 159×10^3 tokens in its KV-cache, testing the Expert Router’s capability to manage models with both a large KV-cache and an efficient data type.

To further improve inference performance, each model incorporates the same optimization techniques. Among these, XQA kernels are employed, which improve Multi-query Attention (MQA) and Grouped-query Attention (GQA) processes during the generation phase [46]. MQA is a modification of the multi-head attention mechanism used in Transformers, where all attention heads share the same set of Key and Value matrices. This design significantly reduces memory bandwidth requirements during incremental inference [53]. GQA modifies the attention mechanism by organizing multiple attention heads into groups, each sharing resources for analyzing segments of the incoming sequences. This structure decreases the number of operations required for processing these sequences [54]. Additionally, all models employ a paged attention mechanism, which enhances the memory efficiency [55].

B. User Simulator

The user simulator manages N synthetic users, sending prompts concurrently to emulate the increasing load on the inference systems. This is accomplished by spawning N independent threads, each functioning independently as a user. These users draw their prompts from a selected segment of the C4 dataset, with a uniform probability distribution across eight categories defined by Gurungan et al. [49] [18]. This ensures an equal distribution of computational workload across the system’s clusters.

The rationale behind the uniform distribution is that it aligns with the scalability of the Expert Router. Such systems can dynamically and autonomously adjust by adding more models to balance spikes in demand for individual clusters, thereby maintaining uniformity in request distribution [56]. The C4 dataset was selected due to its use by Gurungan et al. in developing their k-means clustering algorithm [18]. Each

synthetic user generates a prompt, transmitted to the backend via gRPC, with a token limit of 300 ± 30 . Moreover, each user requests a response prompt of 1200 tokens, a condition enforced by continuous token requests even after the model has indicated sequence completion.

Inference operations are conducted in streaming mode, allowing for measuring the arrival times of individual tokens. This data is stored and later used in the performance evaluation presented in Section V. To simulate a chat scenario, each user sends two sequential prompts to the backend, including the history of the preceding interaction. The initial prompt will be referred to as the "base prompt," while the subsequent prompt will be termed the "continuation prompt." The base prompt contains around 335 ± 30 input tokens, whereas the continuation prompt includes about 1535 ± 30 tokens. This allows to investigate the system under two different load scenarios.

In this study, we increase the number of users from a single user to 1,000 in increments of 100. Furthermore, each run is repeated ten times to measure the uncertainty of the derived metrics.

C. Infrastructure Setup

For all of our experiments, we use a DGX H100. We deploy the Llama 2 70B model in the baseline configuration (A in Table I) through a Triton server, employing tensor parallelization across all eight GPUs. This method is intended to maximize the computational resources available on the DGX system for high-throughput inference tasks.

For the Expert Router experiments, the architecture hosts both the k-means clustering algorithm and individual Triton containers on the same GPUs. Specifically, we deploy 16 instances of the routing gateway, each requiring 1,138 MB of GPU memory, resulting in 2,276 MB on each GPU dedicated to the Expert Router system. The remaining GPU memory is allocated for deploying the individual expert models.

Additionally, the user simulator component is deployed on the CPUs of the same DGX H100 system. By centralizing the experimental setup on a single DGX H100, we aim to reduce potential distortions caused by network latency. However, this approach might lead to interferences among the different components, including the Expert Router, the Triton servers, and the User Simulator, due to the shared use of the system's resources. Such interferences are expected to have a minimal impact on the overall performance metrics.

V. EVALUATION METHODOLOGY

Throughout our experiments, we assess the performance of the Expert Router and the baseline model from two perspectives: user- and system-centric Metrics. This strategy allows us to evaluate system-relevant metrics and analyze the effects of different model configurations on the user interaction latency and throughput.

A. User-Centric Metrics

In the evaluation from the user perspective, we present three metrics. The first is the Time to First Token (TTFT) [19]. It measures the duration from when the user sends a request to when the user receives the first token. We report the TTFT average with increasing number of users. Adjacent to the TTFT, we track the Time Per Output Token (TPOT). It describes the time difference between consecutive tokens. Again, we report the average TPOT for an increasing number of users. Finally, we also investigate the throughput from the user perspective. The user throughput measures the rate at which tokens are received, as experienced by a single user. This metric is calculated by dividing the total number of response tokens by the duration from the request's start (t_s) to the completion of the answer (t_e). We average this value across all users and report the mean and standard deviation.

B. System-Centric Metrics

System-centric metrics evaluate the efficiency and responsiveness of the underlying infrastructure and software as they process tasks, especially when facing a rising number of concurrent user requests. To explore the impact of an increasing number of parallel user requests on system latency, we record the p99 response time for all responses. The p99 response time refers to the 99th percentile response time, meaning that 99% of the requests are processed and responded to within this time frame. This allows us to investigate the effect of the Expert Router on the overall system latency.

Additionally, we adopt two methods to calculate the system's total throughput: session throughput and time-bucket throughput.

Session Throughput: The first approach measures the time it takes for all users to receive their responses in a single session. Again, we use the p99 response time to measure the upper latency bounds under the specific load scenario. The number of users receiving responses within this p99 interval is n_{99} . For this group, we define the session's start and end times by the earliest and latest response times recorded among these users.

$$t_S = \min(t_{s,1}, t_{s,2}, \dots, t_{s,n_{99}}) \quad (1)$$

$$t_E = \max(t_{e,1}, t_{e,2}, \dots, t_{e,n_{99}}) \quad (2)$$

The throughput for a specific number of concurrent users can be calculated by following equation

$$Th_{n_{99}} = \frac{1}{(t_E - t_S)} \sum_{u=1}^{n_{99}} m_u \quad (3)$$

where m_u is the total number of tokens user u received in the answer prompt. The throughput value obtained from Equation 3 enables direct comparison between the different systems deployed in this study. However, this value provides only a broad average, not offering detailed insights into the system's throughput behavior. For a more precise analysis, we track the throughput changes over time.

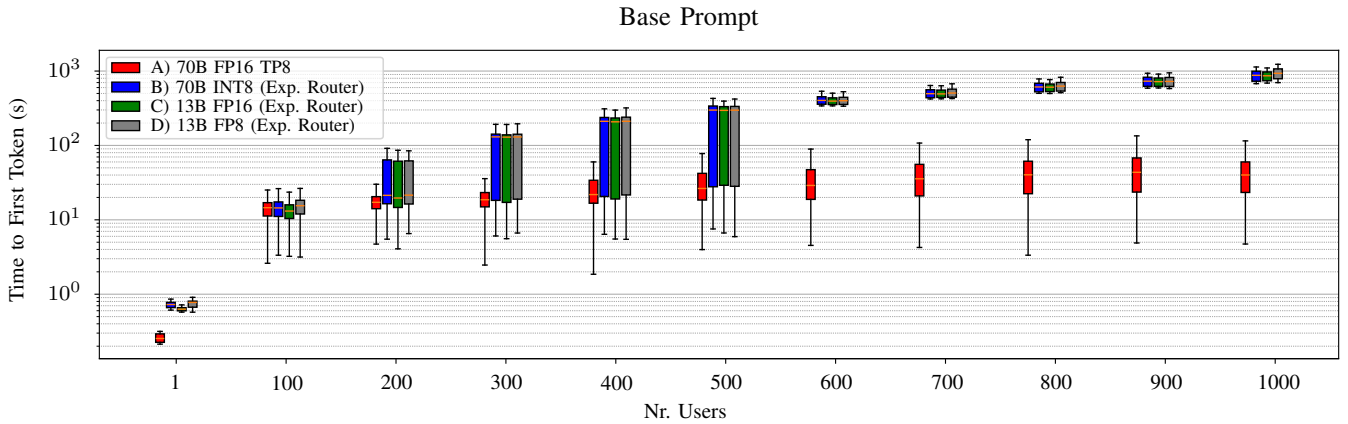


Fig. 2. **Time to First Token for the base prompt:** The models orchestrated via the Expert Router (B-D) exhibit a significantly larger TTFT compared to the tensor parallelized baseline model (A). This is caused by the beneficial parallelized computing of the input sequence by the baseline model (A) during the prefill phase.

Time Bucket Throughput: To add another perspective to our analysis, we assess each trial based on the timestamps associated with all tokens. In each trial, we establish K time intervals (or buckets) and count the number of tokens present within each interval. Thus, we only count how many tokens the system produces in a specific time interval, regardless to which user a specific token belongs. Significantly, this approach does not depend upon the start and end times for the throughput analysis. Equation 3 illustrates that the derived throughput can be significantly influenced by the span between the start and end times. By adopting the time bucket strategy, we mitigate this sensitivity, focusing solely on the distribution of token timestamps.

VI. RESULTS

In this section, we present the outcomes of our experiments, analyzing the performance from both user and system perspectives. To assess the performance of our proposed inference architecture under varied load conditions, we systematically

increased the number of concurrent users sending requests to the system. Additionally, we compare the performance between the base prompt and the continuation prompt.

In addition to the performance metrics presented in Section V we have also measured the latency introduced by the routing gateway. The average latency for each user when sending prompts via the routing gateway is 442 ms with a standard deviation of 302 ms. This high standard deviation is caused by outliers with very high latencies, which could originate from a bottleneck on the DGX system during peak load times. However, as the overall response times for inference are much larger, the latencies introduced by the routing gateway are negligible.

A. User-Centric Metrics

Figure 2 and 3 illustrates the Time-to-First-Token (TTFT) for the base and continuation prompt. The results demonstrate a notable performance gap between the tensor-parallelized baseline model (A) and those orchestrated by the Expert

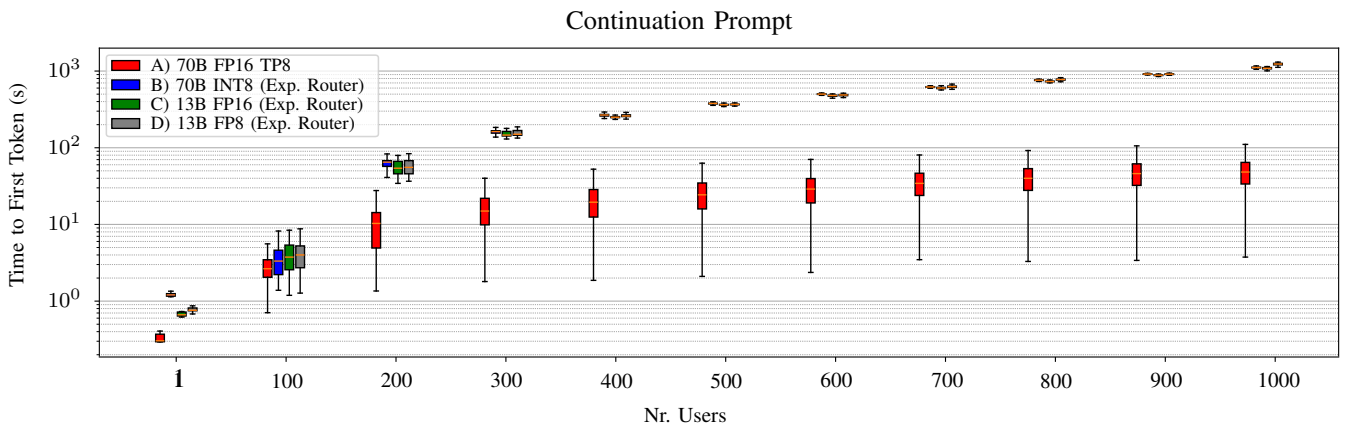


Fig. 3. **Time to First Token for continuation prompt:** Similar to the base prompt, the orchestrated models (B-D) exhibit a significantly higher TTFT compared to the tensor parallelized model (A). No drastic increase of the TTFT between the base and continuation prompt is visible even though the input sequence length has increased.

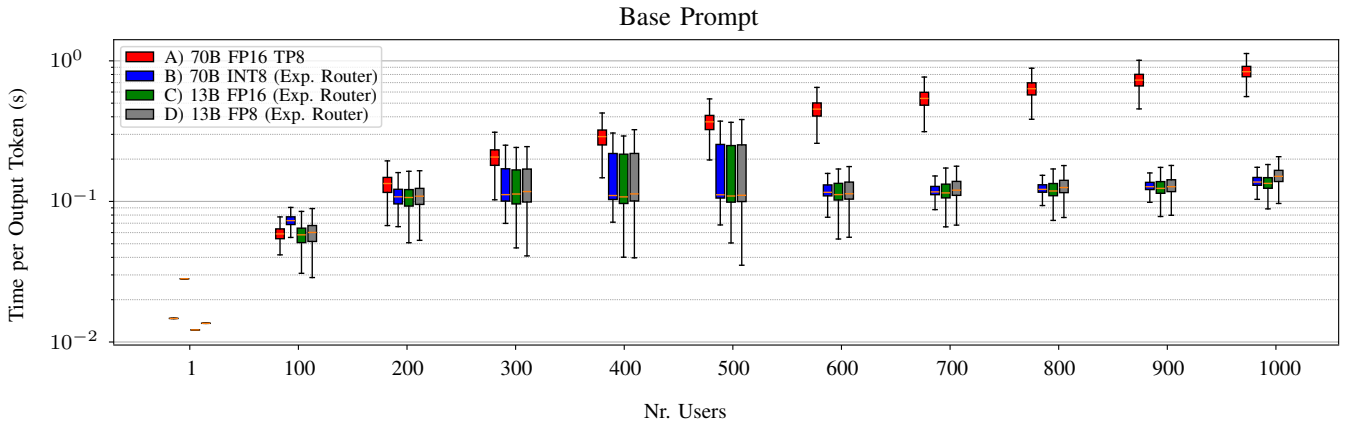


Fig. 4. **Time Per Output Token for the base prompt:** For concurrent user counts above 200, the tensor parallelized baseline model (A) exhibits a higher median TPOT than the orchestrated models (B-D). This can be attributed to the communication cost between the eight GPUs.

Router (B-D). The tensor-parallelized model (A) significantly outperforms the systems orchestrated via the Expert Router. This discrepancy can be attributed to the tensor-parallelized model’s ability to distribute the first stage of inference computations across multiple GPUs. In this stage, the KV-cache is populated by the input’s K and V vectors. This prefill phase involves processing input tokens through a highly parallelizable matrix-matrix multiplication [41]. Each GPU processes a segment of this computation independently and in parallel, and these results are subsequently aggregated through an all-reduce operation for generating the first output token [57]. Due to this parallel execution of the prefill phase, the tensor-parallelized model (A) achieves a significantly shorter TTFT.

The similarity between the base and continuation prompt indicates that the increase in load, due to the increased number of input tokens, does not significantly affect the performance. However, the Expert Router coordinated models (B-D) show decreased variance in the continuation prompt due to this consistent load across all users.

The TTFT advantage of the tensor-parallelized baseline

model (A) turns into a disadvantage for the Time Per Output Token (TPOT) as shown in Figures 4 and 5. Specifically, the TPOT increases for the tensor-parallelized model (A) from 0.1 seconds at 200 users to nearly 1 second at 1000 users for both prompt types. In contrast, the orchestrated models (B-D) maintain a stable TPOT of about 0.1 seconds across user counts. Again, no clear distinction between the different orchestrated models can be seen. By working independently on each GPU, the orchestrated models eliminate the need for inter-GPU communication, thus embracing an embarrassingly parallel framework. This results in a significantly reduced inter-token latency.

Figure 6 evaluates the user throughput in response to increasing system load. This throughput depends on the total response time which can be calculated by $TTFT + TPOT \times N_{r_{tokens}}$. As the number of received tokens is constant, the behavior of the throughput observed by each user only depends on the TTFT and TPOT. Although the tensor-parallelized model (A) demonstrates a notably lower TTFT as the number of users increases, its latency between tokens increases. This

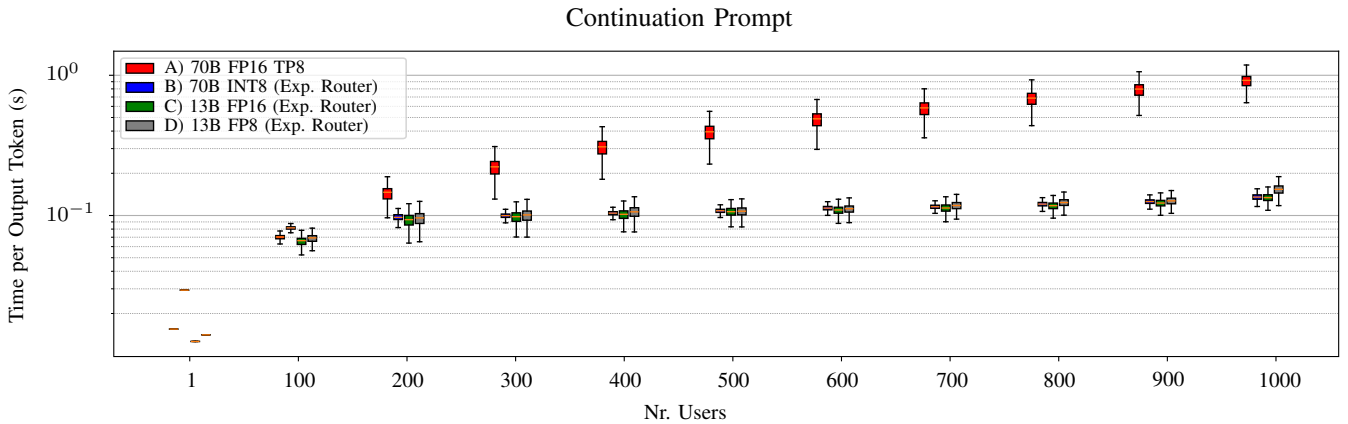


Fig. 5. **Time Per Output Token for the continuation prompt:** Similar to the base prompt, for concurrent user counts above 200, the tensor-parallelized baseline model (A) exhibits a higher TPOT compared to the orchestrated models (B-D).

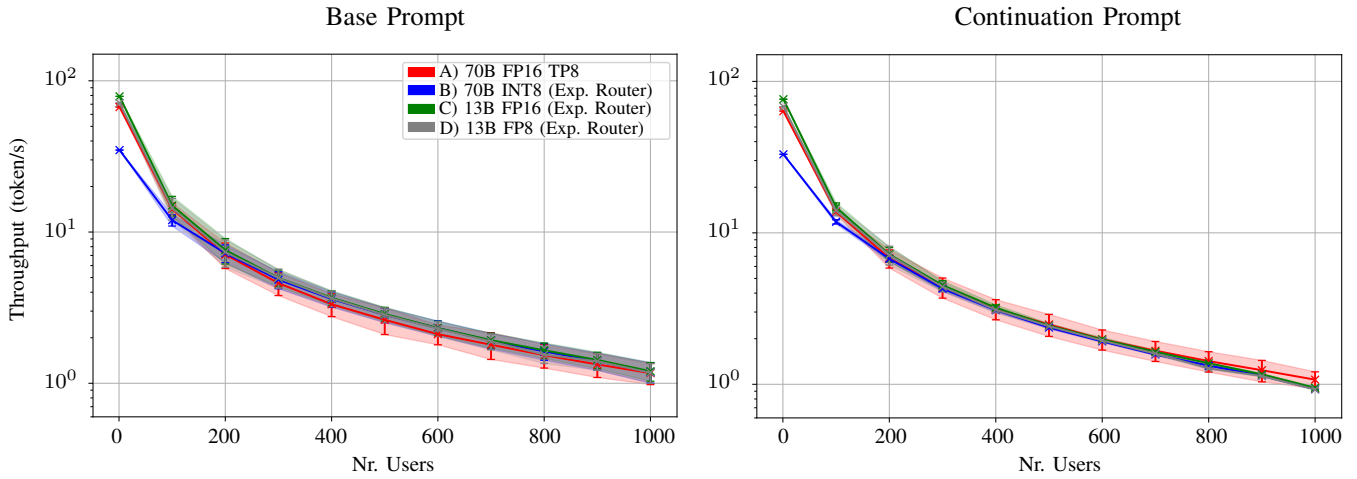


Fig. 6. **User Throughput:** For more than one concurrent user, no clear difference between the models orchestrated by the Expert Router (B-D) and the tensor-parallelized baseline model (A) is visible.

increase in latency results in a throughput that, from the user’s perspective, closely aligns with that of the models orchestrated by the Expert Router (B-D). Conclusively, the scaling of the Expert Router is beneficial in scenarios where many response tokens are required as it increases the total response time less drastically.

B. System-Centric Metrics

In the following, we assess the impact of increasing parallel user requests on the latency measured by the p99 response time and the system throughput. The p99 response time for the base and continuation prompt are illustrated in Figure 7 while the results of the session throughput are shown in Figure 8. In both plots, a performance improvement for the models orchestrated via the Expert Router (B-D) is visible within a range of 200 to 900 Users. To explain this improvement, it is necessary to visualize and investigate the throughput trends over time

shown in Figure 9. In these plots, the throughput is calculated using the time bucket method with time windows of 60 s.

The time bucket throughput across all models is similar at low user numbers (1-100 users) as visible in Figure 9. However, as user numbers increase, the throughput of the tensor-parallelized model (A) exhibits a peak followed by a sharp decline, whereas the orchestrated models (B-D) show multiple peaks, indicating fluctuations between 200 and 2,000 tokens per second. This pattern suggests that the orchestrated models, despite the fluctuations, achieve a more stable and consistent throughput over extended periods, especially as the user count rises.

When the system receives new requests, they are handled by the batcher, which schedules them for processing. This scheduling phase can delay the computation process for generating new output tokens. This initial delay phase, visible for all systems, can be seen as a ramp-up period in Figure 9. It leads to what is referred to as “generation stalls” a decrease in

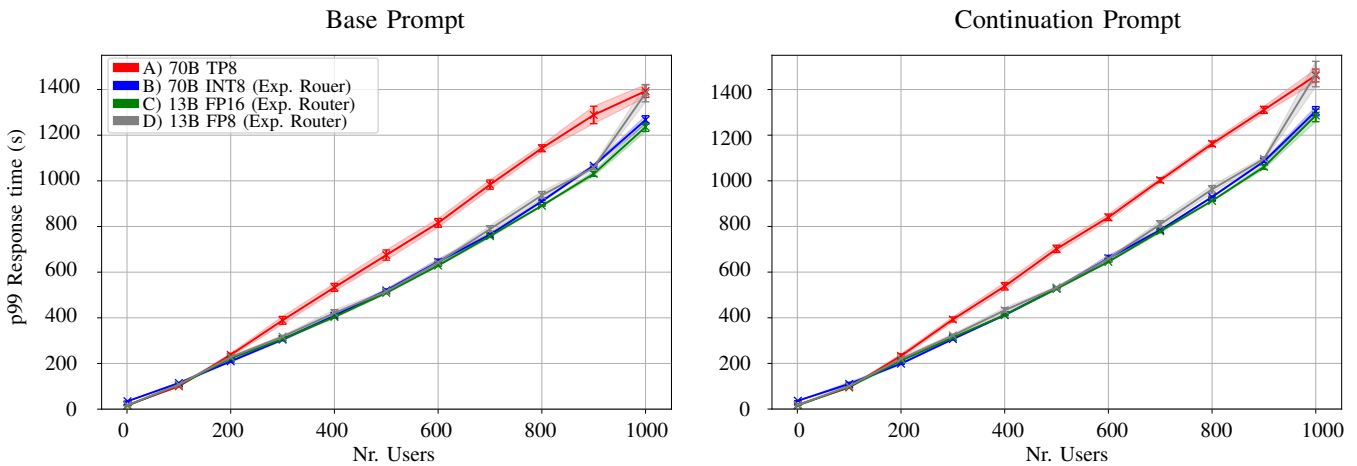


Fig. 7. **p99 Response time:** The p99 response time is smaller for Expert Router orchestrated models (B-D) across user counts of 200-900 compared to the tensor-parallelized baseline model (A).

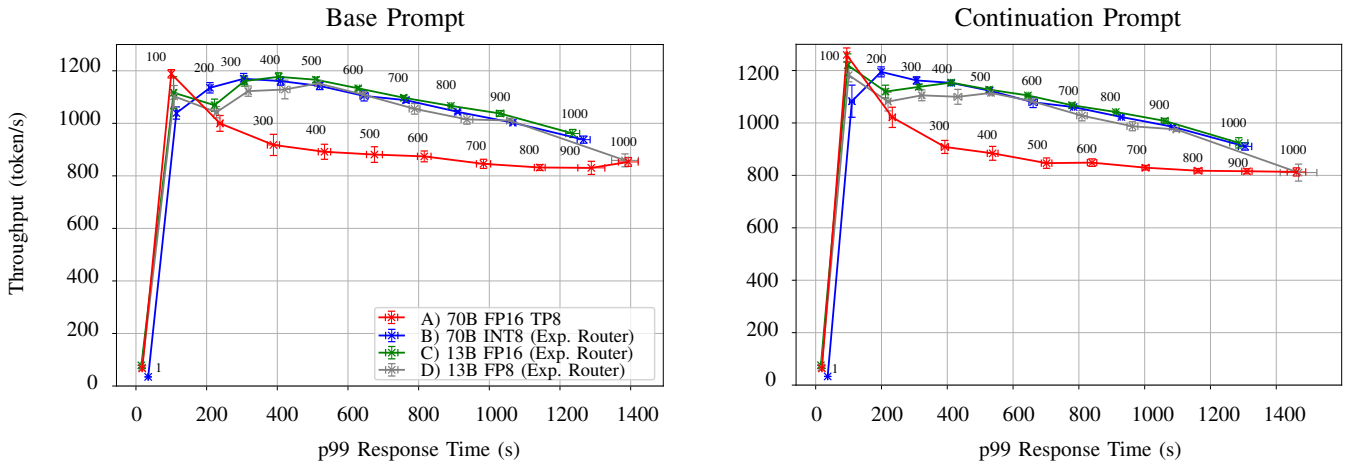


Fig. 8. **Session throughput:** The session throughput, as computed by Equation 3, is higher for Expert Router orchestrated models (B-D) across user counts of 200-900 compared to the tensor-parallelized baseline model (A).

throughput observed during the initial processing stages [41]. For the tensor-parallelized model (A), peak throughput values indicate moments of optimal equilibrium between inter-GPU communication demands and batch processing. On the other hand, the orchestrated models (B-D) process multiple smaller batches concurrently over an extended period, leading to a higher average throughput and more consistent performance. This evidence supports the expert router’s effectiveness, showcasing its ability to enhance system throughput within specific operational ranges.

VII. CONCLUSION AND FUTURE WORK

We introduced Expert Router, a system that efficiently orchestrates multiple specialized LLMs. Through our experimental analysis, we have demonstrated that our orchestration technique maintains throughput comparable to that of a tensor parallelized model and enhances the average system throughput in certain settings. Notably, the parameter count of the

individual experts does not negatively affect the architecture’s performance. As a result, deploying larger quantized models within this framework effectively increases the total parameter count without compromising on system throughput. This advancement opens a new avenue for deploying complex model ensembles in resource-constrained environments, promising improvements in both efficiency and effectiveness.

As part of future work, we plan to create a fully unsupervised pipeline for expert creation and inference. One main focus of this approach will be to conduct a detailed analysis of the model’s ability to generate language, focusing on how different training datasets affect the performance of both the classifier and the expert models. While we used a uniform prompt distribution in this work, one could horizontally scale the number of deployed models for each cluster based on incoming prompts. This would help in keeping an even load across the used infrastructure. Another avenue for future

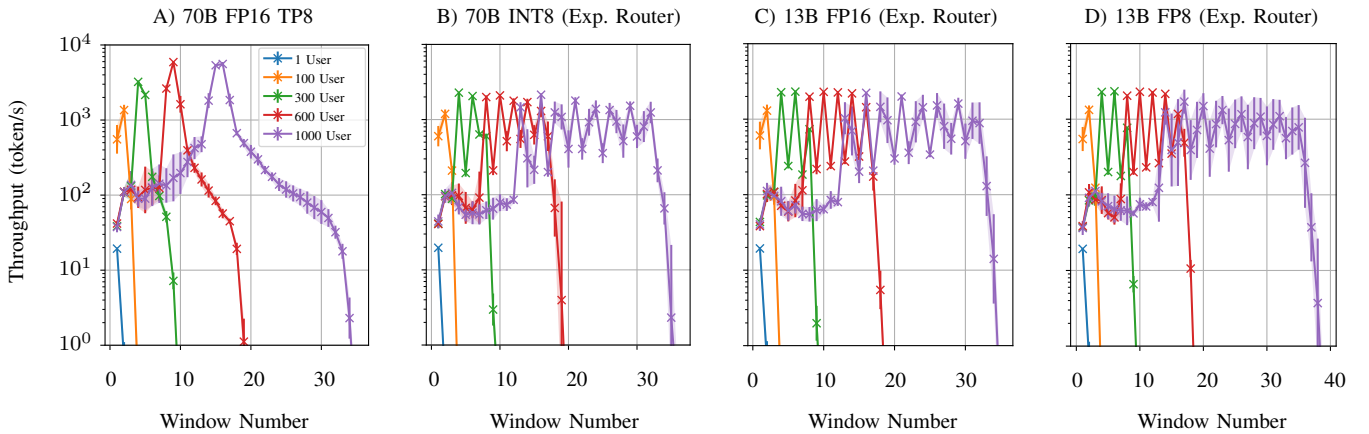


Fig. 9. **Time bucket throughput for the base prompt.** The graphs display the time bucket throughput per model, with time windows of 60s. Each line representing a specific user concurrency level. The tensor-parallelized baseline model (A) exhibits sharp peaks, whereas the models orchestrated by the Expert Router (B-D) demonstrate consistent fluctuations in throughput resulting in a higher average throughput.

exploration is to study if different setups for the Routing Gateway can further increase the performance. Such experiments include testing different embedding and classification algorithms or expanding clustering criteria beyond the prompt domain to incorporate user and request categories.

ACKNOWLEDGMENT

The authors generated parts of this text with OpenAI's language-generation models. Upon generation, the authors reviewed, edited, and revised the language.

REFERENCES

- [1] OpenAI, J. Achiam, S. Adler, S. Agarwal, L. Ahmad, I. Akkaya, F. L. Aleman, D. Almeida, J. Altenschmidt, S. Altman, S. Anadkat, R. Avila, I. Babuschkin, S. Balaji, V. Balcom, P. Baltescu, H. Bao, M. Bavarian, J. Belgum, I. Bello, J. Berdine, G. Bernadett-Shapiro, C. Berner, L. Bogdonoff, O. Boiko, M. Boyd, A.-L. Brakman, G. Brockman, T. Brooks, M. Brundage, K. Button, T. Cai, R. Campbell, A. Cann, B. Carey, C. Carlson, R. Carmichael, B. Chan, C. Chang, F. Chantziis, D. Chen, S. Chen, R. Chen, J. Chen, M. Chen, B. Chess, C. Cho, C. Chu, H. W. Chung, D. Cummings, J. Currier, Y. Dai, C. Decareaux, T. Degry, N. Deutsch, D. Deville, A. Dhar, D. Dohan, S. Dowling, S. Dunning, A. Ecoffet, A. Eleti, T. Eloundou, D. Farhi, L. Fedus, N. Felix, S. P. Fishman, J. Forte, I. Fulford, L. Gao, E. Georges, C. Gibson, V. Goel, T. Gogineni, G. Goh, R. Gontijo-Lopes, J. Gordon, M. Grafstein, S. Gray, R. Greene, J. Gross, S. S. Gu, Y. Guo, C. Hallacy, J. Han, J. Harris, Y. He, M. Heaton, J. Heidecke, C. Hesse, A. Hickey, W. Hickey, P. Hoeschele, B. Houghton, K. Hsu, S. Hu, X. Hu, J. Huizinga, S. Jain, S. Jain, J. Jang, A. Jiang, R. Jiang, H. Jin, D. Jin, S. Jomoto, B. Jonn, H. Jun, T. Kaftan, Lukasz Kaiser, A. Kamali, I. Kanitscheider, N. S. Keskar, T. Khan, L. Kilpatrick, J. W. Kim, C. Kim, Y. Kim, J. H. Kirchner, J. Kiros, M. Knight, D. Kokotajlo, Łukasz Kondraciuk, A. Kondrich, A. Konstantinidis, K. Kosic, G. Krueger, V. Kuo, M. Lampe, I. Lan, T. Lee, J. Leike, J. Leung, D. Levy, C. M. Li, R. Lim, M. Lin, S. Lin, M. Litwin, T. Lopez, R. Lowe, P. Lue, A. Makanju, K. Malfacini, S. Manning, T. Markov, Y. Markovski, B. Martin, K. Mayer, A. Mayne, B. McGrew, S. M. McKinney, C. McLeavey, P. McMillan, J. McNeil, D. Medina, A. Mehta, J. Menick, L. Metz, A. Mishchenko, P. Mishkin, V. Monaco, E. Morikawa, D. Mossing, T. Mu, M. Murati, O. Murk, D. Mély, A. Nair, R. Nakano, R. Nayak, A. Neelakantan, R. Ngo, H. Noh, L. Ouyang, C. O'Keefe, J. Pachocki, A. Paino, J. Palermo, A. Pantuliano, G. Parascandolo, J. Parish, E. Parparita, A. Passos, M. Pavlov, A. Peng, A. Perelman, F. de Avila Belbute Peres, M. Petrov, H. P. de Oliveira Pinto, Michael, Pokorny, M. Pokrass, V. H. Pong, T. Powell, A. Power, B. Power, E. Proehl, R. Puri, A. Radford, J. Rae, A. Ramesh, C. Raymond, F. Real, K. Rimbach, C. Ross, B. Rotsted, H. Roussez, N. Ryder, M. Saltarelli, T. Sanders, S. Santurkar, G. Sastry, H. Schmidt, D. Schnurr, J. Schulman, D. Selsam, K. Sheppard, T. Sherbakov, J. Shieh, S. Shoker, P. Shyam, S. Sidor, E. Sigler, M. Simens, J. Sitkin, K. Slama, I. Sohl, B. Sokolowsky, Y. Song, N. Staudacher, F. P. Such, N. Summers, I. Sutskever, J. Tang, N. Tezak, M. B. Thompson, P. Tillet, A. Tootoonchian, E. Tseng, P. Tuggle, N. Turley, J. Tworek, J. F. C. Uribe, A. Vallone, A. Vijayvergiya, C. Voss, C. Wainwright, J. J. Wang, A. Wang, B. Wang, J. Ward, J. Wei, C. Weinmann, A. Welihinda, P. Welinder, J. Weng, L. Weng, M. Wiethoff, D. Willner, C. Winter, S. Wolrich, H. Wong, L. Workman, S. Wu, J. Wu, M. Wu, K. Xiao, T. Xu, S. Yoo, K. Yu, Q. Yuan, W. Zaremba, R. Zellers, C. Zhang, M. Zhang, S. Zhao, T. Zheng, J. Zhuang, W. Zhuk, and B. Zoph, "Gpt-4 technical report," 2024.
- [2] A. Team, "The claude 3 model family: Opus, sonnet, haiku." https://www-cdn.anthropic.com/de8ba9b01c9ab7cbabf5c33b80b7bbc618857627/Model_Card_Claude_3.pdf, 2024, accessed: 2024-03-31.
- [3] H. Touvron, L. Martin, K. Stone, P. Albert, A. Almahairi, Y. Babaei, N. Bashlykov, S. Batra, P. Bhargava, S. Bhosale, D. Bikel, L. Blecher, C. C. Ferrer, M. Chen, G. Cucurull, D. Esiobu, J. Fernandes, J. Fu, W. Fu, B. Fuller, C. Gao, V. Goswami, N. Goyal, A. Hartshorn, S. Hosseini, R. Hou, H. Inan, M. Kardas, V. Kerkez, M. Khabsa, I. Kloumann, A. Korenev, P. S. Koura, M.-A. Lachaux, T. Lavril, J. Lee, D. Liskovich, Y. Lu, Y. Mao, X. Martinet, T. Mihaylov, P. Mishra, I. Molybog, Y. Nie, A. Poulton, J. Reizenstein, R. Rungta, K. Saladi, A. Schelten, R. Silva, E. M. Smith, R. Subramanian, X. E. Tan, B. Tang, R. Taylor, A. Williams, J. X. Kuan, P. Xu, Z. Yan, I. Zarov, Y. Zhang, A. Fan, M. Kambadur, S. Narang, A. Rodriguez, R. Stojnic, S. Edunov, and T. Scialom, "Llama 2: Open foundation and fine-tuned chat models," 2023.
- [4] R. Bommasani, D. A. Hudson, E. Adeli, R. Altman, S. Arora, S. von Arx, M. S. Bernstein, J. Bohg, A. Bosselut, E. Brunskill, E. Brynjolfsson, S. Buch, D. Card, R. Castellon, N. Chatterji, A. Chen, K. Creel, J. Q. Davis, D. Demszky, C. Donahue, M. Doumbouya, E. Durmus, S. Ermon, J. Etchemendy, K. Ethayarajh, L. Fei-Fei, C. Finn, T. Gale, L. Gillepie, K. Goel, N. Goodman, S. Grossman, N. Guha, T. Hashimoto, P. Henderson, J. Hewitt, D. E. Ho, J. Hong, K. Hsu, J. Huang, T. Icard, S. Jain, D. Jurafsky, P. Kalluri, S. Karamcheti, G. Keeling, F. Khani, O. Khattab, P. W. Koh, M. Krass, R. Krishna, R. Kuditipudi, A. Kumar, F. Ladhak, M. Lee, T. Lee, J. Leskovec, I. Levent, X. L. Li, X. Li, T. Ma, A. Malik, C. D. Manning, S. Mirchandani, E. Mitchell, Z. Munitykwa, S. Nair, A. Narayan, D. Narayanan, B. Newman, A. Nie, J. C. Niebles, H. Nilforoshan, J. Nyarko, G. Ogut, L. Orr, I. Papadimitriou, J. S. Park, C. Piech, E. Portelance, C. Potts, A. Raghunathan, R. Reich, H. Ren, F. Rong, Y. Roohani, C. Ruiz, J. Ryan, C. Ré, D. Sadigh, S. Sagawa, K. Santhanam, A. Shih, K. Srinivasan, A. Tamkin, R. Taori, A. W. Thomas, F. Tramèr, R. E. Wang, W. Wang, B. Wu, J. Wu, Y. Wu, S. M. Xie, M. Yasunaga, J. You, M. Zaharia, M. Zhang, T. Zhang, X. Zhang, Y. Zhang, L. Zheng, K. Zhou, and P. Liang, "On the opportunities and risks of foundation models," 2022.
- [5] M. R. A. H. Rony, C. Suess, S. R. Bhat, V. Sudhi, J. Schneider, M. Vogel, R. Teucher, K. E. Friedl, and S. Sahoo, "Carexpert: Leveraging large language models for in-car conversational question answering," 2023.
- [6] N. Alshahwan, M. Harman, I. Harper, A. Marginean, S. Sengupta, and E. Wang, "Assured llm-based software engineering," 2024.
- [7] N. Gruver, A. Sriram, A. Madotto, A. Wilson, C. L. Zitnick, and Z. Ulissi, "Fine-tuned language models generate stable inorganic materials as text," in *AI for Accelerated Materials Design - NeurIPS 2023 Workshop*, 2023. [Online]. Available: <https://openreview.net/forum?id=0r5DEZ2SwJ>
- [8] J. Clusmann, F. R. Kolbinger, H. S. Muti, Z. I. Carrero, J.-N. Eckardt, N. G. Laleh, C. M. L. Löffler, S.-C. Schwarzkopf, M. Unger, G. P. Veldhuizen, S. J. Wagner, and J. N. Kather, "The future landscape of large language models in medicine," *Communications Medicine*, vol. 3, no. 1, Oct. 2023. [Online]. Available: <https://doi.org/10.1038/s43856-023-00370-1>
- [9] A. Vaswani, N. Shazeer, N. Parmar, J. Uszkoreit, L. Jones, A. N. Gomez, L. u. Kaiser, and I. Polosukhin, "Attention is all you need," in *Advances in Neural Information Processing Systems*, I. Guyon, U. V. Luxburg, S. Bengio, H. Wallach, R. Fergus, S. Vishwanathan, and R. Garnett, Eds., vol. 30. Curran Associates, Inc., 2017.
- [10] P. Liang, R. Bommasani, T. Lee, D. Tsipras, D. Soylu, M. Yasunaga, Y. Zhang, D. Narayanan, Y. Wu, A. Kumar, B. Newman, B. Yuan, B. Yan, C. Zhang, C. Cosgrove, C. D. Manning, C. Ré, D. Acosta-Navas, D. A. Hudson, E. Zelikman, E. Durmus, F. Ladhak, F. Rong, H. Ren, H. Yao, J. Wang, K. Santhanam, L. Orr, L. Zheng, M. Yuksekgonul, M. Suzgun, N. Kim, N. Guha, N. Chatterji, O. Khattab, P. Henderson, Q. Huang, R. Chi, S. M. Xie, S. Santurkar, S. Ganguli, T. Hashimoto, T. Icard, T. Zhang, V. Chaudhary, W. Wang, X. Li, Y. Mai, Y. Zhang, and Y. Koreeda, "Holistic evaluation of language models," 2022.
- [11] S. Yao, D. Yu, J. Zhao, I. Shafran, T. L. Griffiths, Y. Cao, and K. Narasimhan, "Tree of thoughts: Deliberate problem solving with large language models," 2023.
- [12] Q. Wu, G. Bansal, J. Zhang, Y. Wu, B. Li, E. Zhu, L. Jiang, X. Zhang, S. Zhang, J. Liu, A. H. Awadallah, R. W. White, D. Burger, and C. Wang, "Autogen: Enabling next-gen llm applications via multi-agent conversation framework," 2023.
- [13] J. Hoffmann, S. Borgeaud, A. Mensch, E. Buchatskaya, T. Cai, E. Rutherford, D. de Las Casas, L. A. Hendricks, J. Welbl, A. Clark, T. Hennigan, E. Noland, K. Millican, G. van den Driessche, B. Damoc, A. Guy, S. Osindero, K. Simonyan, E. Elsen, J. W. Rae, O. Vinyals, and L. Sifre, "Training compute-optimal large language models," 2022.
- [14] Y. Li, S. Bubeck, R. Eldan, A. D. Giorno, S. Gunasekar, and Y. T. Lee, "Textbooks are all you need ii: phi-1.5 technical report," September 2023. [Online]. Available: <https://www.microsoft.com/en-us/research/publication/textbooks-are-all-you-need-ii-phi-1-5-technical-report/>
- [15] W. Fedus, J. Dean, and B. Zoph, "A review of sparse expert models in deep learning," 2022.

- [16] Y. Zhou, T. Lei, H. Liu, N. Du, Y. Huang, V. Zhao, A. Dai, Z. Chen, Q. Le, and J. Laudon, "Mixture-of-experts with expert choice routing." [Online]. Available: <http://arxiv.org/abs/2202.09368>
- [17] Y. Wang, K. Chen, H. Tan, and K. Guo, "Tabi: An efficient multi-level inference system for large language models," in *Proceedings of the Eighteenth European Conference on Computer Systems*, ser. EuroSys '23. New York, NY, USA: Association for Computing Machinery, 2023, p. 233–248. [Online]. Available: <https://doi.org/10.1145/3552326.3587438>
- [18] S. Gururangan, M. Li, M. Lewis, W. Shi, T. Althoff, N. A. Smith, and L. Zettlemoyer, "Scaling expert language models with unsupervised domain discovery," 2023.
- [19] X. Miao, G. Oliaro, Z. Zhang, X. Cheng, H. Jin, T. Chen, and Z. Jia, "Towards efficient generative large language model serving: A survey from algorithms to systems." [Online]. Available: <http://arxiv.org/abs/2312.15234>
- [20] W. Fedus, B. Zoph, and N. Shazeer, "Switch transformers: Scaling to trillion parameter models with simple and efficient sparsity." [Online]. Available: <http://arxiv.org/abs/2101.03961>
- [21] A. Q. Jiang, A. Sablayrolles, A. Roux, A. Mensch, B. Savary, C. Bamford, D. S. Chaplot, D. d. l. Casas, E. B. Hanna, F. Bressand, G. Lengyel, G. Bour, G. Lample, L. R. Lavaud, L. Saulnier, M.-A. Lachaux, P. Stock, S. Subramanian, S. Yang, S. Antoniak, T. L. Scao, T. Gervet, T. Lavril, T. Wang, T. Lacroix, and W. E. Sayed, "Mixtral of experts." [Online]. Available: <http://arxiv.org/abs/2401.04088>
- [22] X. Nie, X. Miao, S. Cao, L. Ma, Q. Liu, J. Xue, Y. Miao, Y. Liu, Z. Yang, and B. Cui, "EvoMoE: An evolutionary mixture-of-experts training framework via dense-to-sparse gate." [Online]. Available: <http://arxiv.org/abs/2112.14397>
- [23] C. N. d. Santos, J. Lee-Thorp, I. Noble, C.-C. Chang, and D. Uthus, "Memory augmented language models through mixture of word experts." [Online]. Available: <http://arxiv.org/abs/2311.10768>
- [24] C.-H. Lee, H. Cheng, and M. Ostendorf, "OrchestraLLM: Efficient orchestration of language models for dialogue state tracking." [Online]. Available: <http://arxiv.org/abs/2311.09758>
- [25] R. Krishnamoorthi, "Quantizing deep convolutional networks for efficient inference: A whitepaper," 2018.
- [26] S. Ma, H. Wang, L. Ma, L. Wang, W. Wang, S. Huang, L. Dong, R. Wang, J. Xue, and F. Wei, "The era of 1-bit LLMs: All large language models are in 1.58 bits." [Online]. Available: <http://arxiv.org/abs/2402.17764>
- [27] J. Lin, J. Tang, H. Tang, S. Yang, X. Dang, C. Gan, and S. Han, "AWQ: Activation-aware weight quantization for LLM compression and acceleration." [Online]. Available: <http://arxiv.org/abs/2306.00978>
- [28] G. Xiao, J. Lin, M. Seznec, H. Wu, J. Demouth, and S. Han, "SmoothQuant: Accurate and efficient post-training quantization for large language models." [Online]. Available: <http://arxiv.org/abs/2211.10438>
- [29] T. Dettmers, M. Lewis, Y. Belkada, and L. Zettlemoyer, "LLM.int8(): 8-bit matrix multiplication for transformers at scale." [Online]. Available: <http://arxiv.org/abs/2208.07339>
- [30] E. Frantar, S. Ashkboos, T. Hoeffer, and D. Alistarh, "GPTQ: Accurate post-training quantization for generative pre-trained transformers." [Online]. Available: <http://arxiv.org/abs/2210.17323>
- [31] R. Pope, S. Douglas, A. Chowdhery, J. Devlin, J. Bradbury, A. Levskaia, J. Heck, K. Xiao, S. Agrawal, and J. Dean, "Efficiently scaling transformer inference." [Online]. Available: <http://arxiv.org/abs/2211.05102>
- [32] B. Wu, Y. Zhong, Z. Zhang, G. Huang, X. Liu, and X. Jin, "Fast distributed inference serving for large language models." [Online]. Available: <http://arxiv.org/abs/2305.05920>
- [33] Z. Liu, J. Wang, T. Dao, T. Zhou, B. Yuan, Z. Song, A. Shrivastava, C. Zhang, Y. Tian, C. Re, and B. Chen, "Deja vu: Contextual sparsity for efficient LLMs at inference time." [Online]. Available: <http://arxiv.org/abs/2310.17157>
- [34] J. Hagemann, S. Weinbach, K. Dobler, M. Schall, and G. de Melo, "Efficient parallelization layouts for large-scale distributed model training." [Online]. Available: <http://arxiv.org/abs/2311.05610>
- [35] vLLM Development Team, "vllm: Easy, fast, and cheap llm serving with pagedattention," <https://vllm.ai>, 2023.
- [36] O. R. developers, "Onnx runtime," <https://onnxruntime.ai/>, 2021.
- [37] NVIDIA Corporation, "Triton inference server: An optimized cloud and edge inferencing solution." [Online]. Available: <https://github.com/triton-inference-server/server>
- [38] A. Paszke, S. Gross, S. Chintala, G. Chanan, E. Yang, Z. DeVito, Z. Lin, A. Desmaison, L. Antiga, and A. Lerer, "Automatic differentiation in pytorch," 2017.
- [39] R. Y. Aminabadi, S. Rajbhandari, M. Zhang, A. A. Awan, C. Li, D. Li, E. Zheng, J. Rasley, S. Smith, O. Ruwase, and Y. He, "DeepSpeed inference: Enabling efficient inference of transformer models at unprecedented scale." [Online]. Available: <http://arxiv.org/abs/2207.00032>
- [40] HuggingFace, "Text generation inference," <https://huggingface.co/text-generation-inference>.
- [41] A. Agrawal, N. Kedia, A. Panwar, J. Mohan, N. Kwatra, B. S. Gulavani, A. Tumanov, and R. Ramjee, "Taming throughput-latency tradeoff in LLM inference with sarathi-serve." [Online]. Available: <http://arxiv.org/abs/2403.02310>
- [42] Reproducible performance metrics for LLM inference. [Online]. Available: <https://www.anyscale.com/blog/reproducible-performance-metrics-for-llm-inference>
- [43] V. J. Reddi, C. Cheng, D. Kanter, P. Mattson, G. Schmuelling, C.-J. Wu, B. Anderson, M. Breughe, M. Charlebois, W. Chou, R. Chukka, C. Coleman, S. Davis, P. Deng, G. Damos, J. Duke, D. Fick, J. S. Gardner, I. Hubara, S. Idgunji, T. B. Jablin, J. Jiao, T. S. John, P. Kanwar, D. Lee, J. Liao, A. Lokhmotov, F. Massa, P. Meng, P. Micikevicius, C. Osborne, G. Pekhimenko, A. T. R. Rajan, D. Sequeira, A. Sirasao, F. Sun, H. Tang, M. Thomson, F. Wei, E. Wu, L. Xu, K. Yamada, B. Yu, G. Yuan, A. Zhong, P. Zhang, and Y. Zhou, "MLPerf inference benchmark." [Online]. Available: <http://arxiv.org/abs/1911.02549>
- [44] MLCommons. MLPerf results Highlight Growing Importance of Generative AI and Storage. <https://mlcommons.org/2023/09/mlperf-results-highlight-growing-importance-of-generative-ai-and-storage/>.
- [45] "ray-project/llmperf," original-date: 2023-10-10T16:49:58Z. [Online]. Available: <https://github.com/ray-project/llmperf>
- [46] NVIDIA/TensorRT-LLM. [Online]. Available: <https://github.com/NVIDIA/TensorRT-LLM/tree/main>
- [47] gRPC Authors, "grpc," 2023, accessed: 2024-03-29. [Online]. Available: <https://grpc.io/>
- [48] F. Pedregosa, G. Varoquaux, A. Gramfort, V. Michel, B. Thirion, O. Grisel, M. Blondel, P. Prettenhofer, R. Weiss, V. Dubourg, J. Vanderplas, A. Passos, D. Cournapeau, M. Brucher, M. Perrot, and E. Duchesnay, "Scikit-learn: Machine learning in Python," *Journal of Machine Learning Research*, vol. 12, pp. 2825–2830, 2011.
- [49] C. Raffel, N. Shazeer, A. Roberts, K. Lee, S. Narang, M. Matena, Y. Zhou, W. Li, and P. J. Liu, "Exploring the limits of transfer learning with a unified text-to-text transformer." [Online]. Available: <http://arxiv.org/abs/1910.10683>
- [50] W. Reese, "Nginx: the high-performance web server and reverse proxy," *Linux J.*, vol. 2008, no. 173, sep 2008.
- [51] G.-I. Yu, J. S. Jeong, G.-W. Kim, S. Kim, and B.-G. Chun, "Orca: A distributed serving system for Transformer-Based generative models," in *16th USENIX Symposium on Operating Systems Design and Implementation (OSDI 22)*. Carlsbad, CA: USENIX Association, Jul. 2022, pp. 521–538. [Online]. Available: <https://www.usenix.org/conference/osdi22/presentation/you>
- [52] Using FP8 with transformer engine — transformer engine 1.4.0 documentation. [Online]. Available: https://docs.nvidia.com/deeplearning/transformer-engine/user-guide/examples/fp8_primer.html
- [53] N. Shazeer, "Fast transformer decoding: One write-head is all you need." [Online]. Available: <http://arxiv.org/abs/1911.02150>
- [54] J. Ainslie, J. Lee-Thorp, M. de Jong, Y. Zemlyanskiy, F. Lebrón, and S. Sanghai, "GQA: Training generalized multi-query transformer models from multi-head checkpoints." [Online]. Available: <http://arxiv.org/abs/2305.13245>
- [55] W. Kwon, Z. Li, S. Zhuang, Y. Sheng, L. Zheng, C. H. Yu, J. Gonzalez, H. Zhang, and I. Stoica, "Efficient memory management for large language model serving with PagedAttention," in *Proceedings of the 29th Symposium on Operating Systems Principles*, ser. SOSP '23. Association for Computing Machinery, pp. 611–626. [Online]. Available: <https://dl.acm.org/doi/10.1145/3600006.3613165>
- [56] D. Buchaca, J. L. Berral, C. Wang, and A. Youssef, "Proactive container auto-scaling for cloud native machine learning services," in *2020 IEEE 13th International Conference on Cloud Computing (CLOUD)*, 2020, pp. 475–479.
- [57] M. Shoeybi, M. Patwary, R. Puri, P. LeGresley, J. Casper, and B. Catanzaro, "Megatron-LM: Training multi-billion parameter

language models using model parallelism.” [Online]. Available:
<http://arxiv.org/abs/1909.08053>